Spring 5-9-2020

glucose metabolism of breast cancer sub-clones that preferentially metastasize to the lungs and bone

Anna G. Skubiz
University of Mississippi

GLUCOSE METABOLISM OF BREAST CANCER SUB-CLONESS THAT PREFERENTIALLY METASTASIZE TO THE LUNGS AND BONE

By
Anna Grace Skubiz

A Thesis Submitted to The University in Mississippi in partial fulfillment of the requirements of the Sally McDonnell Barksdale Honors College.

Oxford
May 2020

Approved By:

_____
Advisor: Dr. Mika Jekabsons

_____
Reader: Dr. Susan Pedigo

_____
Reader: Dr. Colin Jackson

AWKNOWLEDGEMENTS

I would like to thank Dr. Mika Jekabsons for his mentorship. I am grateful for the opportunity to have performed research in his lab. I have learned to be a better researcher and student because of him. I would most like to thank him for his patience, support, and encouragement for my project as well as my future endeavors. I would also like to thank Mollie Merrell, Noah Thornton, and Blake Raboin for their assistance with this project and their support. I appreciate both Dr. Susan Pedigo and Dr. Colin Jackson for their time committed to this project. Finally, I would like to thank my family and friends for their support and encouragement over the years dedicated to this project.

ABSTRACT

ANNA GRACE SKUBIZ: The Effect of Glutamine on Metabolism of Metastasis in Different Organ Microenvironments.
(Under the direction of Dr. Mika Jekabsons)

Malignant breast cancers exhibit preferential metastasis to bone and lung (1). While changes in gene expression in lung-specific (LM) and bone-specific metastasis (BoM) lines derived from the MDA-MB-231 breast cancer line have been identified, few metabolic genes are differentially expressed; thus it is unknown if tissue-specific metabolic reprogramming occurs. Two hallmarks of cancer cells are an altered metabolic phenotype characterized by enhanced conversion of glucose to lactate in spite of adequate oxygen availability for complete mitochondrial oxidation of this substrate (referred to as aerobic glycolysis or the Warburg effect) and a greater dependence on glutamine. These changes in primary tumor metabolism are crucial for cancer cell metastasis by increasing the supply of glycolytic and tricarboxylic acid (TCA) cycle intermediates that are necessary for de novo biosynthetic pathways. I hypothesize that the LM and BoM lines exhibit metabolic reprogramming to allow for proliferation in the lung and bone microenvironments, respectively. The rates of glucose consumption, mitochondrial respiration, and lactate production were determined for MDA-MB-231, LM, BoM, and the less aggressive T47D lines given either glucose or glucose and glutamine as the exogenous substrates. Aerobic glycolysis for the BoM and LM lines, was greater than the MDA231 and T47D lines. Respiration rate was significantly lower in the BoM and LM lines. Glutamine consumption normalized to glucose consumption was significantly lower for BoM cells, suggesting this line has a lower preference for glutamine. Glutamine had significant main effects on glucose uptake, lactate production, and a near significant

effect on aerobic glycolysis; the effect of glutamine on mitochondrial respiration was cell line dependent, as this substrate tended to reduce T47D and MDA231 respiration while increasing it in LM cells. These data indicate that the LM and BoM sub-clones have different metabolic phenotypes than the parent MDA-MB-231 cells and the extent of the differences is affected by glutamine. Further, the LM and BoM phenotypes differ from each other given their responses to exogenous glutamine. Successful growth of metastatic cells from a primary tumor in secondary organs such as lung and bone may thus require metabolic plasticity characterized by higher aerobic glycolysis and lower mitochondrial activity.

TABLE OF CONTENTS

List of Figures

List of Abbreviations

LM	Lung-specific metastasis
BoM	Bone-specific metastasis
MDA	MDA-MB-231 Metastatic breast cancer line
TCA	Tricarboxylic acid
T47D	Control breast cancer line
HIF	Hypoxia-inducible factor
GLUT	Glucose transporter
AMPK	Adenosine monophosphate-activated protein kinase
ROS	Reactive oxygen species
IDH	Isocitrate dehydrogenase
FH	Fumarate hydratase
SDH	Succinate dehydrogenase
VDAC	Voltage dependent ion channel
TGFβ	Transforming growth factor
ATP	Adenosine triphosphate
NADP	Nicotinamide adenine dinucleotide phosphate
NAD	Nicotinamide adenine dinucleotide
NADPH	Nicotinamide adenine dinucleotide phosphate
α-KG	α-ketoglutarate
Ri5P	Ribose 5 phosphate
PYR	Pyruvate
FA	Fatty acid

INTRODUCTION

Transcriptomic studies have identified unique gene expression profiles in sub-clones of metastatic tumors that preferentially invade different organs (1). Individual cells within the MDA-MB-231 metastatic breast cancer line have unique gene expression profiles and thus are genetically heterogeneous. Such heterogeneity contributes to the probability of invasion of the lungs, bone, and brain (2). Specific genes that mediate breast cancer metastasis to the bones and lungs (3) have been identified that facilitate one or more of the following processes of metastasis: intravasation, adhesion, extravasation, angiogenesis, and finally growth in a distant tissue (2). Notably, a prerequisite for successful growth in a distant tissue is a metabolic infrastructure capable of meeting the demands for substrates and energy in an environment that may differ from the tissue in which the original tumor developed (***Fig. 1***). There is evidence that triple negative breast cancer cells such as the MDA-MB-231 line have the capacity to adjust their metabolic phenotype upon detachment from the primary tumor (4). However, it is unclear if unique metabolic adaptations occur as metastatic cells invade different secondary organs.

Cells that detach from the primary tumor and circulate in the blood have changes in metabolism, specifically increases in mitochondrial biogenesis and respiration.

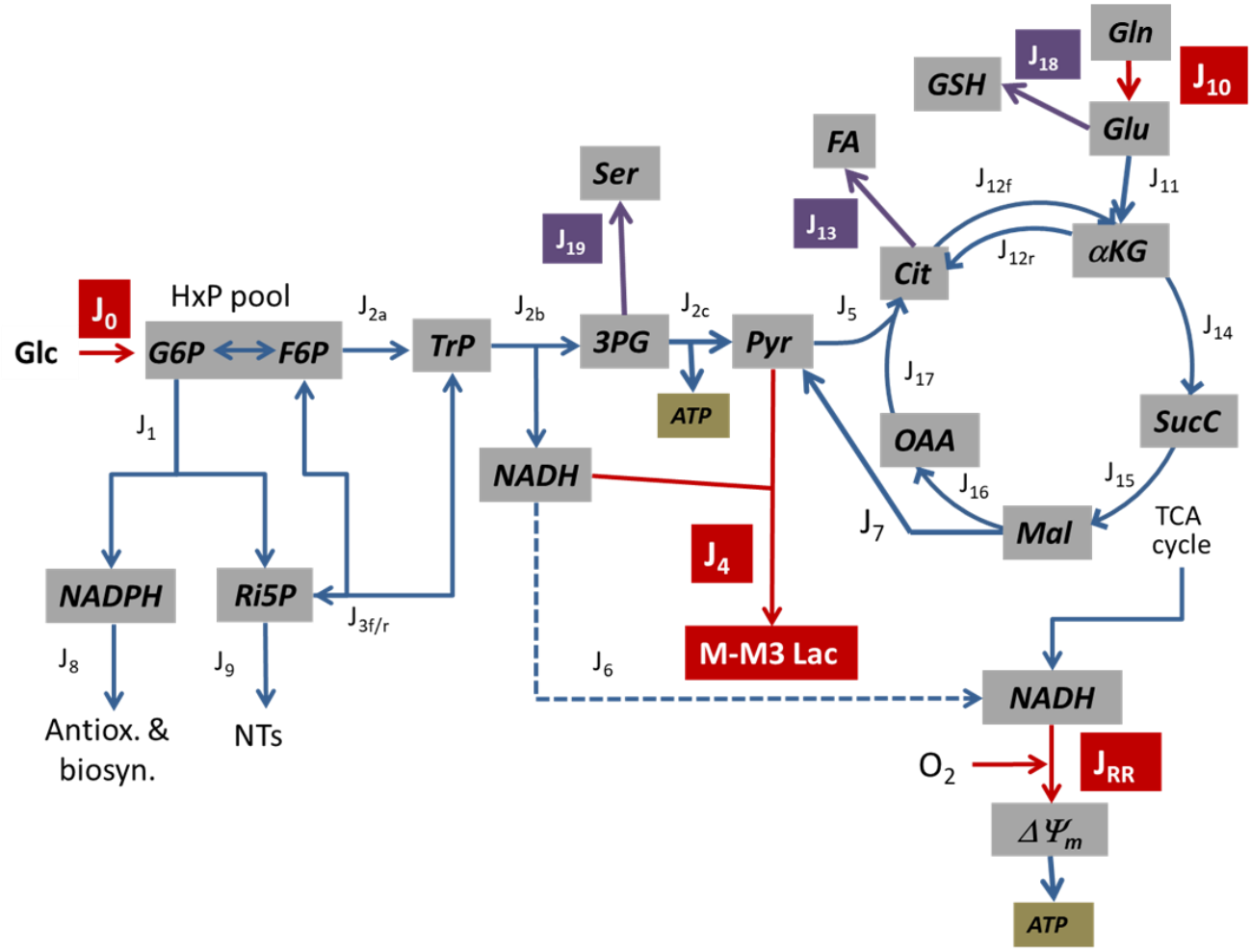

Figure 1: Diagram of glycolysis and the tricarboxylic acid cycle. Notable intermediates are given. J_0, J_4, J_{10}, and J_{RR} were the measured fluxes for glucose consumption, lactate production, glutamine consumption, and respiration rate which were the focuses of this experiment.

This indicates that cells leaving the primary tumor have differing metabolic properties that may depend on the immediate environment (4). While glucose and glutamine are important for growth of most cancers, the pathways through which these substrates are processed may change with the microenvironment (***Fig. 1***). The fraction of glucose used

for the pentose phosphate pathway, fatty acid synthesis, or oxidation by mitochondria can vary depending on reactive oxygen species (ROS) production, availability and uptake capacity of exogenous fatty acids, and the degree of mitochondrial dysfunction. Similarly, the fraction of glutamine used for protein, glutathione, or fatty acid synthesis, and for oxidation by the tricarboxylic acid (TCA) cycle and/or malic enzyme can vary depending on ROS production and availability of other substrates. The number of tumorigenic genes that contribute to metabolic changes seen in cancer has yet to be resolved (5), but hypoxia inducible factor-1 (HIF-1) has a major role as a 'master regulator' of glucose metabolism. It promotes glycolytic activity by upregulating glucose transporters (GLUT) and multiple glycolytic genes. HIF-1, in coordination with AMP activated protein kinase (AMPK), regulates glucose uptake used for glycolysis and the TCA cycle. The variations in HIF-1 and AMPK activities, together with mitochondrial reactive oxygen species (ROS) signaling, can lead to metabolic plasticity in cancer and may partly explain the differences in glucose and glutamine uptake, lactate production, and mitochondrial respiration observed in different cancers. This has been shown in breast cancer cells having high expression of HIF-1 and AMPK that produce lactate at a higher rate compared to benign cells (4). Specifically, HIF-1α is responsive in cancer cell hallmarks such as angiogenesis but is also highly involved in metabolism (6).

MDA-MB-231 gene expression exhibits a typical poor prognosis signature that is associated with metastasis and resistance to radiation and chemotherapy. In vivo, such a gene expression signature is thought to occur in only a small percentage of cells within the breast tumor (1). Although a tumor may carry the poor prognosis signature, it is proposed that organ specific metastasis is determined by different sets of genes (7). The isolation of highly lung-, bone-, and brain-specific metastatic subclones from the MDA231 cells has allowed progress on the mechanisms driving tissue-specific metastasis. To date, most of the work has centered on gene expression differences but this provides limited insight into the physiological differences between cells of the primary tumor and those growing in secondary organs. The transformation of breast epithelial cells to the metastatic MDA-MB-231 line involves changes in expression of multiple metabolic genes, including isocitrate dehydrogenases-1 and -2 (IDH1, IDH2), fumarate hydratase (FH), and the succinate dehydrogenase (SDH) complex. Additionally, expression of voltage-dependent anion channel 1 (VDAC1), which allows for metabolite and ROS exchange between mitochondria and cytoplasm, is essential for the growth of cancer cells such as MDA. This demonstrates that coordinated changes to the expression of metabolic genes are important for the physiology of cancer cells in general and furthermore subtle changes may be important for the lung, bone and brain metastatic subclones, but no metastatic preferences have been noted (6).

Primary tumors that metastasize to different organs over- or under-express a common set of genes, including COX2, MMP1, ANGPTL4, LTPB1 (controls TGFβ activation), FSCN1, and RARRES3. Breast cancers that often metastasize to the lungs (3) overexpress COX2 and MMP1 along with 48 other genes mentioned in the Minn study. The most notable of this group are ID1, CXCL1, along with COX2 and MMP1 because they are directly and almost exclusively correlated with lung metastasis. These genes assist in invasion through mediation of cell signaling and intracellular modulation of gene expression. Additionally, a decrease in ID1, VCAM1, or IL13Rα2 has been shown to drastically decrease preferential metastasis to lung (7). It is unclear how the majority of overexpressed genes are involved in facilitating lung metastasis, and notable that none of the identified genes have a role in glucose or glutamine metabolism. There are similar numbers of overexpressed genes unique to bone metastasis; furthermore, there is limited overlap in which genes aid the invasion of bone and lung tissue (3). CXCR4, CXCL12 and RANKL are overexpressed in breast cancers that metastasize to bone; the latter two are known to stimulate mammary tumor growth (5). CXCL12 is a regulator of hematopoiesis and has been proposed to regulate the immune system to influence metastasis. IL11 and OPN overexpression significantly increase MDA-MB-231 metastasis to bone. There is a proposition that TGFβ may further stimulate this metastasis, contrary to its expected role as a tumor suppressor. TGFβ increases already

overexpressed IL11 and CTGF in populations highly metastatic to bone further supporting tumor progression (8). While many of these genes have a role in cell signaling (7), the impact on metabolism remains unknown.

One of the most unique metabolic properties of cancer cells is the Warburg effect. Otto Warburg found that even in the presence of oxygen, cancer cells ferment glucose to lactate (the glycolytic index) at extremely high rates (17). This effect is thought to be important to increase supply of glycolytic intermediates for different biosynthetic pathways. Further, glutamine is consumed at a rate one to two orders of magnitude higher than in untransformed cells (9). It is essential for the survival and proliferation of most cancer cells by sustaining both ATP synthesis and biosynthetic pathways (10, 11). In 1955 it was found that proliferating tumor cells have a high demand for glutamine (9). The focus of this research is to identify the metabolic differences that may exist between cell lines in the absence or presence of glutamine and the impact glutamine makes on metabolic processes.

METHODS

A. Cell lines and culture

Metastatic breast cancer MDA-MB-231 cells (hereafter referred to as MDA231) and the less aggressive T47D breast cancer cells were provided by Dr. Y.D. Zhou (University of Mississippi, Department of Chemistry and Biochemistry). Sub-clones of MDA231 cells that preferentially metastasize in lung (LM) and bone (BoM) were generated by Massague's lab (12, 13). Both LM and BoM cells were obtained from Dr. Kounosuke Watabe (Wake Forest University) and provided by Dr. Zhou. Cells were routinely cultured using RPMI-1640 media supplemented with 10% fetal bovine serum and 0.5% vol/vol penicillin-streptomycin in 10 cm polystyrene petri dishes at 37^{o}C in a humidified 5% CO_2 incubator. Cells were maintained in culture for no more than 20 passages, and typically split twice a week. The day before each experiment, approximately 1.0 x 10^6 cells were seeded in each well of 2-well Lab-Tek chambers. Control wells received 2mL standard cell culture media while treatment wells were incubated in glutamine-free RPMI-1640 media supplemented with 1.5 mM 5-^{13}C glutamine. Cells were incubated for 20-22 hours prior to experiments.

B. Materials

Glutamate pyruvate transaminase, glucose-6-phosphate dehydrogenase (G6PDH), lactate dehydrogenase, nicotinamide adenine dinucleotide phosphate (NADP), nicotinamide

adenine dinucleotide (NAD), adenosine triphosphate (ATP), and 2 oxoglutarate were purchased from Calzyme (San Luis Obispo, CA). Hexokinase and microbial glutamate dehydrogenase were purchased from Sigma (St. Louis, MO). Glutaminase was purchased from Megazyme (Chicago, IL). 5-^{13}C glutamine was purchased from Cambridge Isotopes (Tewksbury, MA). Cell culture media, fetal bovine serum, and cell culture supplies were purchased from Fisher Scientific (Pittsburg, PA). Buffers and other general reagents were purchased from Sigma.

C. Flux experiments

After overnight incubation in cell culture media ± 5-^{13}C glutamine, cells were rinsed then equilibrated 5 h 37^{o}C in experimental buffer containing 137 mM NaCl, 5 mM KCl, 20 mM TES, 1.3 mM $CaCl_2$, 1.3 mM $MgCl_2$, 1.2 mM Na_2SO_4, 0.4 mM KH_2PO_4, 0.2 mM $NaHCO_3$, 5.5 mM glucose, 0.3 % fatty acid-free bovine serum albumin (BSA), ± 1.5 mM 5-^{13}C glutamine, pH 7.4. The control buffer contained no glutamine. Respiration rate of cells in each well was determined at 37^{o}C in 2.15 mL fresh buffer using a custom-made setup with a Clark-type micro-oxygen electrode (Micrelectrodes, Inc., Bedford MA) (***Fig. 2***. Data for each well was acquired over 45-55 min. with a Powerlab A/D unit and Lab Chart software (AD Instruments). Cells were rinsed once with buffer then serially incubated for 60 min, 120 min, and 60 min at 37^{o}C with 350 μL buffer. After each incubation period, buffer was collected in microfuge tubes on ice, the cells were rinsed once, and then 350 μL buffer added for the next incubation period. Control wells without cells were incubated in parallel to correct for evaporative volume changes over each incubation period. The samples were centrifuged for 5 min. 4^{o}C at 21,000 xg and supernatants stored at -20^{o}C for metabolite assays. The 60 min incubations were used to

assess average rates of glucose consumption and lactate production, while all three were used to assess glutamine consumption. Cell pellets were visible for the MDA231 samples; these were saved and assayed for protein content to correct for protein loss over each incubation period. After the final incubation, wells were rinsed once with 1 ml phosphate buffered saline (PBS) then solubilized for 15 min at 37°C with 500 µL 50 mM NaCl, 20 mM TES, 1% SDS, pH 7.3. The extracts were vortexed 2-3 min. then centrifuged 10 min. 21,000xg 10°C and the supernatants stored at -20°C for protein assay. The MDA231 cell pellets were washed once with 200 µL PBS, repelleted by centrifugation, then solubilized with 100 µL SDS buffer and stored at -20°C.

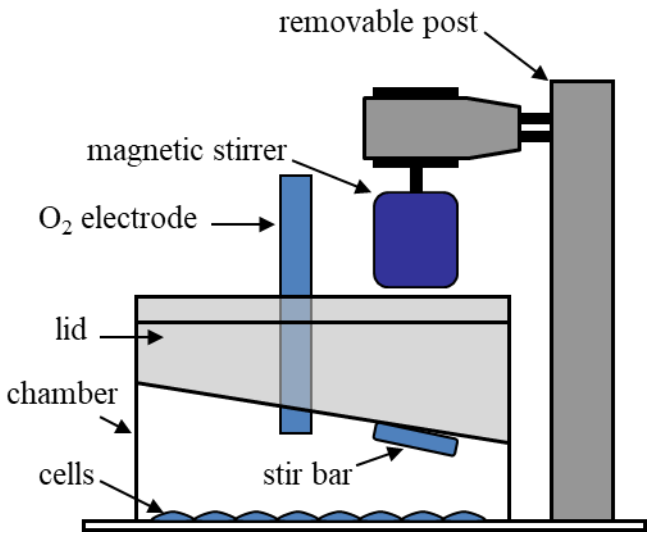

Figure 2: Set up for respiration measurement. Shown are the cells plated at the bottom of chamber. A stir bar located in the media is being turned by a magnetic stirrer on the other side of the cell chamber lid. In the container is an O_2 electrode which measures the decreasing oxygen concentration of the buffer.

D. Metabolite assays

D.1. Glucose Assay

Buffer glucose concentrations were determined by enzymatic assay. Samples (5 µl) were run in triplicate in assay buffer (115 µl) containing 100mM triethanolamine, 7 mM

$MgCl_2$, 2 mM ATP, 2 mM NADP, 1 U/mL glucose-6-phosphate dehydrogenase, 1 U/mL hexokinase, pH 7.3. Following a 10min incubation, fluorescence was quantitated using a Shimadzu RF-6000 spectrofluorophotometer (λ_{ex}=341 nm, λ_{em}=464 nm, excitation and emission slits 5nm and 15nm, respectively). Glucose standards (3.5, 4.0, 4.5, 5.0, 5.5, and 6.0 mM) were prepared in experimental buffer and run in parallel.

D.2. Glutamine Assay

Glutamine concentrations were determined by a two-step enzymatic reaction. For the first reaction, duplicate samples (6 µL) were incubated 45 min at 37^{o}C in reaction buffer (34 µL) containing 60 mM sodium acetate, with or without 1 U/mL glutaminase, pH 4.5. Reactions without glutaminase served as controls to quantitate background ammonia production by the cells, which was subtracted to obtain the glutamine-derived ammonia. The second reaction was initiated by adding 80 µL of 300 mM Tris, 10 mM 2-oxoglutarate, 240 µM NADPH, and 2 U/mL microbial L-glutamate dehydrogenase, pH 8.5 to each sample. After 60 min incubation protected from light, fluorescence was quantitated using a Shimadzu RF-6000 spectrofluorophotometer (λ_{ex}=341 nm, λ_{em}=464 nm, excitation and emission slits of 10nm). Glutamine standards (0, 0.2, 0.4, 0.8, 1.2, 1.6, and 2.0 mM) were prepared in experimental buffer and run in parallel.

D.3. Lactate Assay

Buffer lactate concentrations were determined by enzymatic assay. Samples (5 µL) were run in triplicate in assay buffer (115 µL) containing 100 mM glycylglycine, 100 mM glutamate, 2 mM NAD, 1 U/mL lactate dehydrogenase, and 1 U/mL glutamate pyruvate transaminase, pH 8.5. Following a 40min incubation fluorescence was quantitated using a

Shimadzu RF-6000 spectrofluorophotometer (λ_{ex}=341 nm, λ_{em}=464 nm, excitation and emission slits 15nm and 20nm, respectively). Lactate standards (0, 0.5, 1.0, 1.5, 2.0, and 2.5 mM) were prepared in experimental buffer and run in parallel.

D.4. Protein Assay

Quantitation of total protein in soluble cell extracts (duplicates, diluted 1:3 in water) were determined by bicinchoninic acid (BCA) assay. Reactions (25 µl sample with 500 µl BCA reagent) were incubated for 30 min, 60^{o}C, cooled, and quantitated at 562 nm using a Ultrospec 3100pro spectrophotometer (Amersham Biosciences). Bovine serum albumin standards (0, 50, 100, 150, 200, 300, 400, and 500 ug/ml) dissolved in solubilization buffer were run in parallel. Additionally, protein assays were run for the MDA cell pellets to correct for protein lost over each incubation period. The MDA cells have a much lower adherence to the plate than the three other lines. Due to this inequality MDA cells were spun into pellets and assayed to measure the protein content as a form of compensation to account for the cell loss during the experiment.

D.5. Statistics

For each variable, two-way analysis of variance (ANOVA) was run to assess main effects of cell line and treatment (glutamine) and cell line x treatment interaction. When significant main effects of cell line were observed, differences between the cell lines within a treatment (i.e., either with or without glutamine) were assessed by one-way-ANOVA with Tukey's post-hoc test. Significant effects of glutamine on a particular cell line were assessed by paired T-test. $P<0.05$ was taken as the level of significance.

RESULTS

Table 1: 2-way ANOVA p-values for the main effects of treatment (± glutamine), cell line, and treatment x cell line interaction for the measured variables.

	Treatment	Cell line	Interaction
Glucose uptake	0.0231	<0.0001	0.2832
Lactate production	0.0005	<0.0001	0.3166
Lac/Glc	0.0585	<0.0001	0.26
Respiration rate	0.2108	<0.0001	0.015
RR/Glc	0.0263	<0.0001	0.4197
Protein	0.2881	<0.0001	0.9142

A. Glucose uptake

Glucose is a primary substrate used by tumor cells for energy homeostasis by ATP synthesis, redox homeostasis by NADPH and NADH synthesis, and for anabolic processes such as nucleotide, fatty acid, and amino acid synthesis. The rate of glucose uptake is thus an important indicator of overall tumor cell metabolism. For all experiments, glucose concentrations decreased anywhere from 0.5-2.0 mM, so the concentrations did not change by more than about 40% of the initial concentration (5.5 mM). Since the Km for GLUT1, the most prevalent glucose transporter, is about 1-2 mM, this change should have little effect on uptake rate, so the rates were calculated assuming steady-state conditions over each 60 min. period.

Without glutamine present, glucose uptake rate was, as anticipated, significantly lower for the least aggressive, slow growing T47D cells than the three metastatic lines (***Fig. 3***).

LM and BoM uptake rates were not different (p=0.39), but both were significantly lower than the parent MDA231 cells. In the presence of glutamine, all four cell lines differed significantly from each other. Glutamine tended to decrease glucose uptake in three of the lines, which accounts for the significant main effect of glutamine treatment on glucose uptake (***Table 1***); BoM and MDA231 cells tended to have lower rates of glucose uptake (p=0.14 and p=0.07, respectively by paired t-test with no glutamine treatment) while T47D uptake was significantly lower (p=0.01). The LM uptake rate was insensitive to glutamine, and this together with the tendency toward lower BoM uptake resulted in a significant difference (p=0.002) between these lines (***Fig. 3***. These data suggest that the LM and BoM sub-clones may have a different metabolic phenotype than the parent MDA231 cells from which they were derived, and the extent of this difference is affected by glutamine.

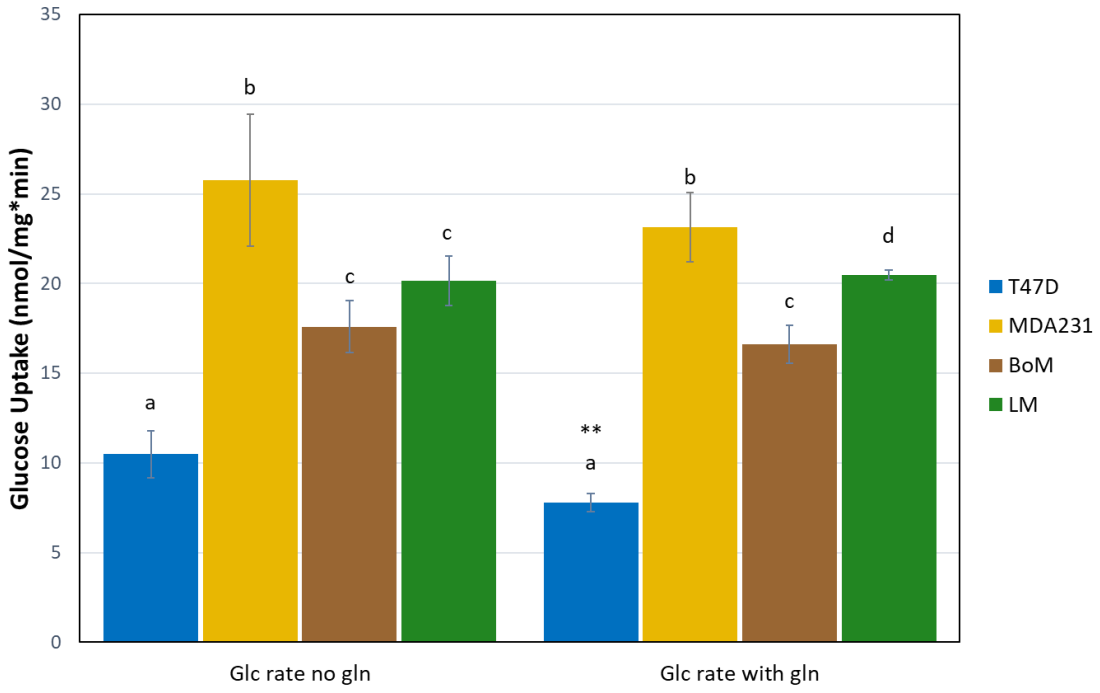

Figure 3: Glucose uptake for each cell line incubated with or without glutamine. Buffer glucose concentrations were determined by enzymatic assay and rates averaged over two 60 min. incubations. Rates were normalized to total SDS-soluble protein. Data are mean ± standard error (n=4). Within a treatment, means sharing the same letter are not significantly different. Asterisks above a letter denote significant difference with the corresponding cell line in glutamine-free buffer.

B. Lactate production

Lactate is a primary end product of glucose metabolism that is produced at greater rates when oxygen becomes limiting for mitochondrial oxidative phosphorylation and hence is an indicator of anaerobic metabolism. However, cancer cells have been found to produce more lactate than untransformed cells, even when oxygen is not limiting for oxidative phosphorylation. This is known as the Warburg effect or more commonly aerobic glycolysis. Lactate production has been linked to metastasis formation, evasion of immune response, angiogenesis and chemoresistance (14). These traits, unique to cancer cells have made lactate production a key indicator of metastatic progression. For these experiments, lactate accumulation ranged from 0.5-2.5 mM over the 60 min. incubations. The rates of efflux were assumed to be constant over this time period, but the higher

concentrations accumulated in some experiments with LM cells could negatively affect efflux rate given that the rate and direction of transport by the monocarboxylate transporter depends partly on the plasma membrane lactate gradient.

Without glutamine, differences in lactate production were similar to that of glucose consumption. The more metastatic MDA231, BoM and LM lines produced lactate at a 2-3 fold greater rate than T47D cells (***Fig.4)***. LM rate was between and not different from either the MDA231 ($p=0.53$) or BoM ($p=0.10$) lines, while the latter two lines differed significantly ($p=0.01$). In the presence of glutamine, T47D, MDA231, and LM lactate production decreased significantly, whereas BoM rate was unchanged. The lower MDA231 and LM rates resulted in no differences between the three aggressive metastatic lines. This suggests that the rates of aerobic glycolysis in these three lines may be the same. Additionally, the effect of glutamine may indicate that MDA231 and LM lines rely more on this substrate for ATP synthesis by oxidative phosphorylation than BoM cells.

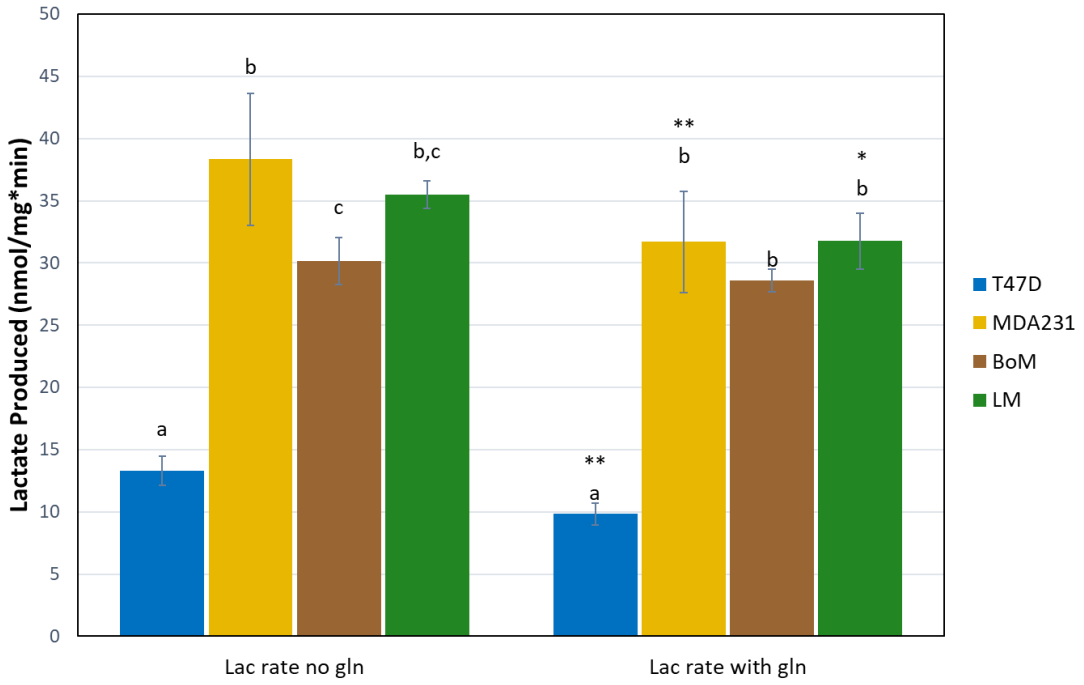

Figure 4: Lactate production rate for each cell line incubated with or without glutamine. Buffer lactate concentrations were determined by enzymatic assay and rates averaged over two 60 min. incubations. Rates were normalized to total SDS-soluble protein. Data are mean ± standard error (n=4). Within a treatment, means sharing the same letter are not significantly different. Asterisks above a letter denote significant difference with the corresponding cell line in glutamine-free buffer.

Lactate production provides an absolute estimate of aerobic glycolysis, but normalizing lactate production to glucose consumption reports the proportion of glucose converted to lactate, known as the glycolytic index, and is a better measure of comparing aerobic glycolysis between cell lines. Cancer cells are known to have a higher glycolytic index than untransformed cells, possibly to support tumor growth by increasing the supply of glycolytic intermediates used for anabolic reactions. More aggressive, metastatic tumors typically have a higher glycolytic index. Without glutamine, this was the case (***Fig. 5***); furthermore, the LM and BoM ratios were significantly, or borderline significantly, higher than the parent MDA231 line. Glutamine did not affect the T47D or BoM ratios, either because the cells were insensitive to glutamine (BoM) or both glucose consumption and lactate production were reduced proportionally (T47D). The MDA231 and LM glycolytic indexes were lower (although not significantly, p=0.12 and p=0.07,

respectively), with the latter most affected because glutamine reduced lactate production without affecting glucose uptake (***Figs. 3 and 4***); this explains this near-significant (p=0.06) main effect of glutamine (***Table 1***). Somewhat surprisingly, the MDA231 index did not differ from T47D cells (p=0.58), whereas LM and BoM cells remained significantly greater. These data suggest that the BoM and LM lines convert a greater proportion of the glucose they consume to lactate, and hence have a higher 'normalized' aerobic glycolysis than the MDA231 line.

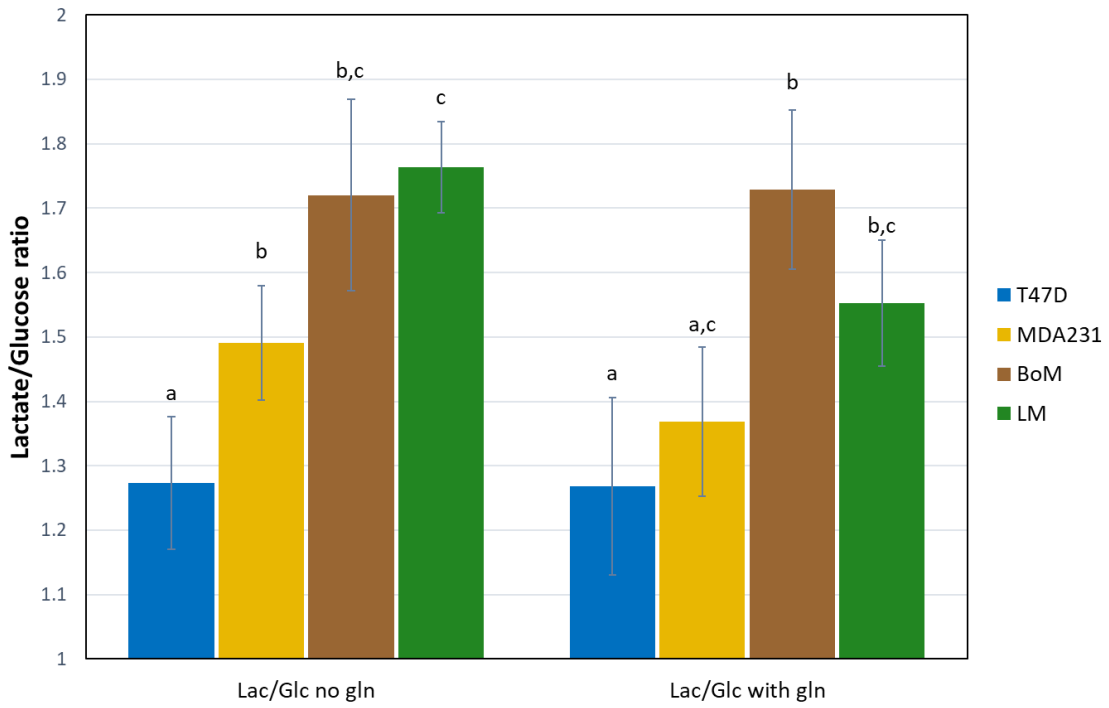

Figure 5: The lactate to glucose ratio, otherwise known as the glycolytic index, shown across cell lines with and without glutamine. The buffer concentration was determined by taking data from the previous graphs into a ratio. Rates were normalized to total SDS-soluble protein. Data are mean ± standard error (n=4). Within a treatment, means sharing the same letter are not significantly different. Asterisks above a letter denote significant difference with the corresponding cell line in glutamine-free buffer.

C. Mitochondrial Respiration Rate

Respiration rate of cells attached to the bottom of the Lab-Tek chambers was measured with a custom oxygen electrode setup prior to incubations to determine glucose, lactate,

and glutamine rates (***Fig. 2)***. Mitochondrial respiration rate was determined by subtracting non-mitochondrial oxygen consumption that had been previously determined in Seahorse Extracellular Flux Analyzer experiments as rotenone plus antimycin A insensitive rates (Y.D. Zhou, personal communication; for T47D, MDA231, BoM, and LM lines, the fraction that was non-mitochondrial was 0.23±0.01, 0.11±0.02, 0.09±0.05, and 0.23±0.05, respectively; mean±standard error, n=8). Since the oxygen consumed is used at the end of the electron transport chain as an electron acceptor, and the electrons are derived from substrates oxidized within the mitochondrial matrix, respiration rate is an indirect measure of substrate oxidation rate in this organelle.

Without glutamine, respiration rate differed significantly among all four lines. Surprisingly, the greatest differences were between the MDA231 cells and the LM/BoM sub-clones, which had 3-4-fold lower rates (***Fig. 6***). While there was no significant main effect of glutamine on respiration rate, the treatment x cell line interaction was significant (***Table 1***). This was the result of glutamine tending to stimulate LM ($p=0.12$) but reduce T47D ($p=0.06$) and MDA ($p=0.14$) respiration. Because of the stimulation by glutamine, LM and BoM rates were not different, but significantly lower than the T47D and MDA231 rates. It is interesting to note that glutamine tended to lower the lactate: glucose ratio for both MDA231 and LM cells, suggesting lower anaerobic glycolysis, but oppositely affected LM and MDA231 mitochondrial activity. This data does imply that the sub-clones of MDA231 rely far less on oxidative phosphorylation as a source of ATP

than the parent line.

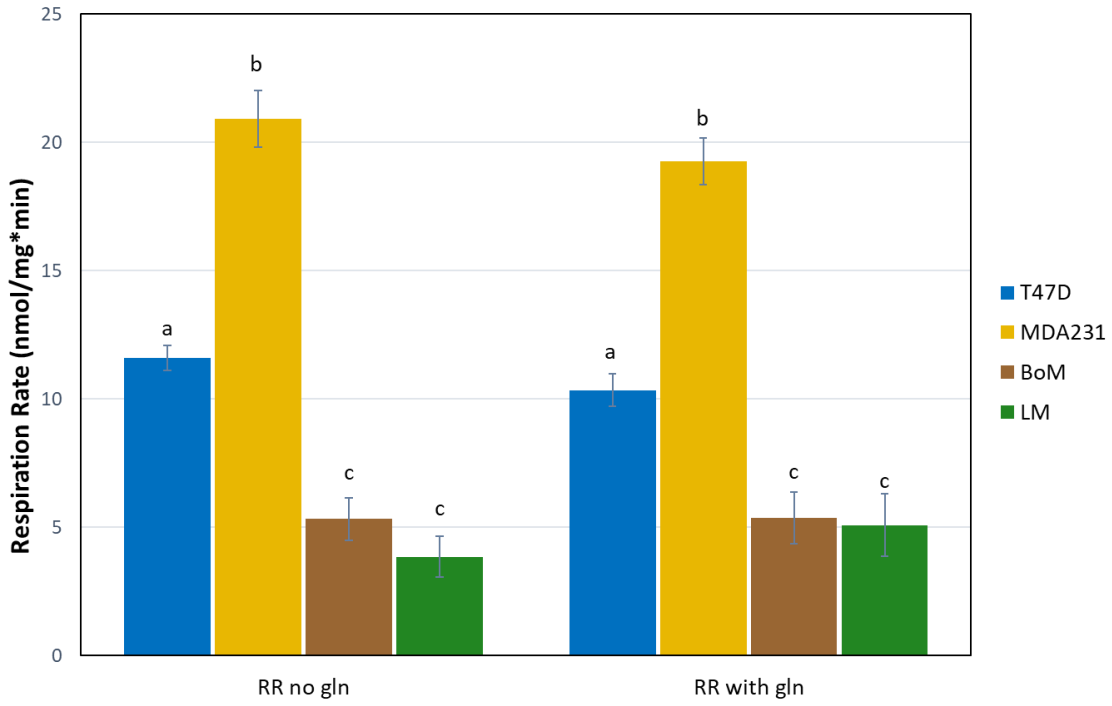

Figure 6: Cellular respiration rate for each cell line incubated with or without glutamine. Buffer oxygen concentrations were determined through apparatus measurements, rates averaged over two 60 min. incubations. Rates were normalized to total SDS-soluble protein. Data are mean ± standard error (n=4). Within a treatment, means sharing the same letter are not significantly different. Asterisks above a letter denote significant difference with the corresponding cell line in glutamine-free buffer.

Respiration rate normalized to glucose uptake provides an assessment complementary to the lactate: glucose ratio on the glycolytic index of different cell lines. For cells that divert more glucose to lactate, less mitochondrial activity might be expected since relatively more ATP will be supplied by glycolysis; cells with higher lactate: glucose ratio are thus predicted to have a lower respiration: glucose ratio. In general, this prediction held true for these four cell lines, both with or without glutamine. The T47D line, which had the lowest lactate: glucose ratio, had the highest respiration rate to glucose ratio. MDA231 is the second highest ratio (***Fig. 7***). Conversely, the BoM and LM lines having the highest lactate: glucose ratios had the lowest respiration rate: glucose ratios. These data further suggest that the lung and bone metastatic sub-clones have

greater anaerobic glycolysis and lower oxidative phosphorylation than the parent MDA231 line.

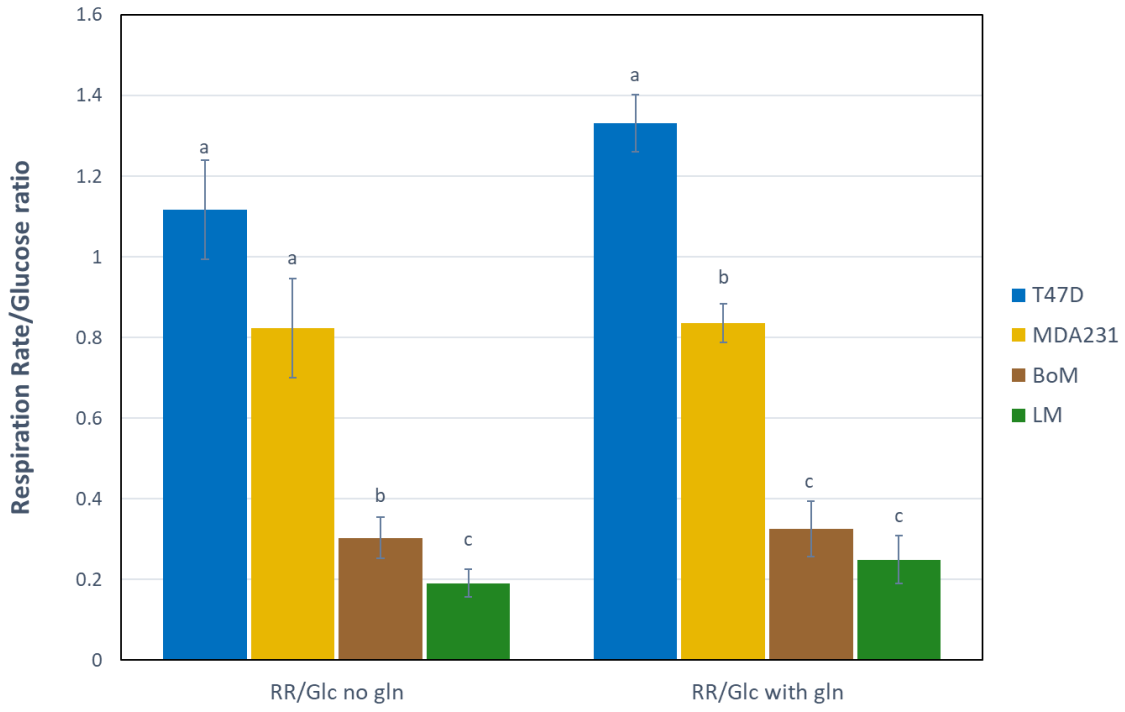

Figure 7: This figure shows the respiration rate to glucose ratio. The buffer concentration was determined by taking data from the previous graphs into a ratio. Rates were normalized to total SDS-soluble protein. Data are mean ± standard error (n=4). Within a treatment, means sharing the same letter are not significantly different. Asterisks above a letter denote significant difference with the corresponding cell line in glutamine-free buffer.

D. Glutamine Uptake

Glutamine, like glucose, can be used for ATP, nucleotide, fatty acid, and amino acid/protein synthesis. Cancer cells are known to consume excess glutamine compared to other cells, to support these more active anabolic processes. A main fate of glutamine is to mitochondria for supply of TCA cycle intermediates citrate, malate, and oxaloacetate. Glutamine uptake is generally much lower than the rate of glucose consumption, so for these assays 120 min incubations were also used to ensure detectable changes in glutamine concentrations. Since the rates assessed over 120 min were similar to that over 60 min, these were averaged to obtain the uptake rates.

Glutamine uptake was highest in the MDA231and LM lines. Surprisingly, BoM uptake was significantly lower and no different from T47D cells despite the more glycolytic, proliferative phenotype of the BoM line (***Fig. 8***).

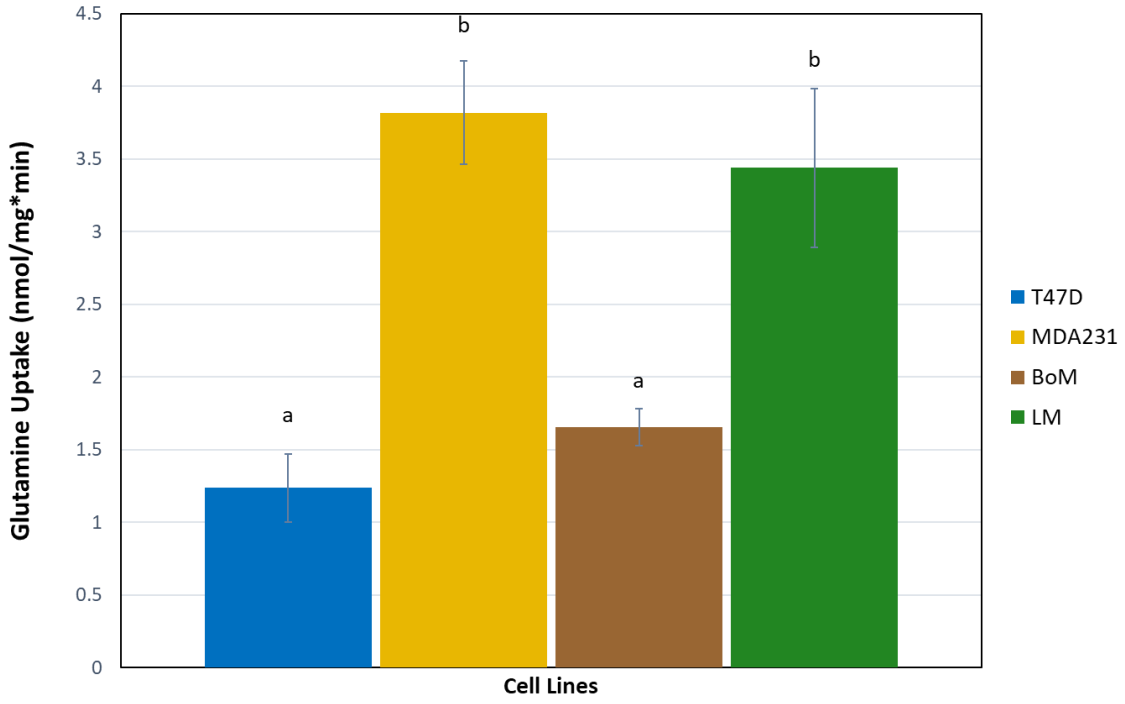

Figure 8: Glutamine uptake rate for each cell line incubated with glutamine. Buffer glutamine concentrations were determined through enzymatic assay, rates averaged over two 60 min. incubations. Rates were normalized to total SDS-soluble protein. Data are mean ± standard error (n=4). Within a treatment, means sharing the same letter are not significantly different. Asterisks above a letter denote significant difference with the corresponding cell line in glutamine-free buffer.

Glutamine rates were normalized to glucose rates to assess the relative importance of glutamine as a substrate. The more rapidly proliferating LM and BoM lines were predicted to have higher glutamine: glucose ratios given the importance of glutamine in supporting multiple anabolic pathways. Contrary to the prediction, the BoM ratio was significantly lower while the T47D line was no different from the more aggressive MDA231 and LM lines (***Fig. 9***). These data suggest that the more metastatic lines do not have a greater preference for glutamine.

There is no significant difference in the glutamine to glucose ratio of T47D, LM, or MDA cells. BoM cells are the exception in this measurement being the only line considered to have a different level of glutamine to glucose consumption.

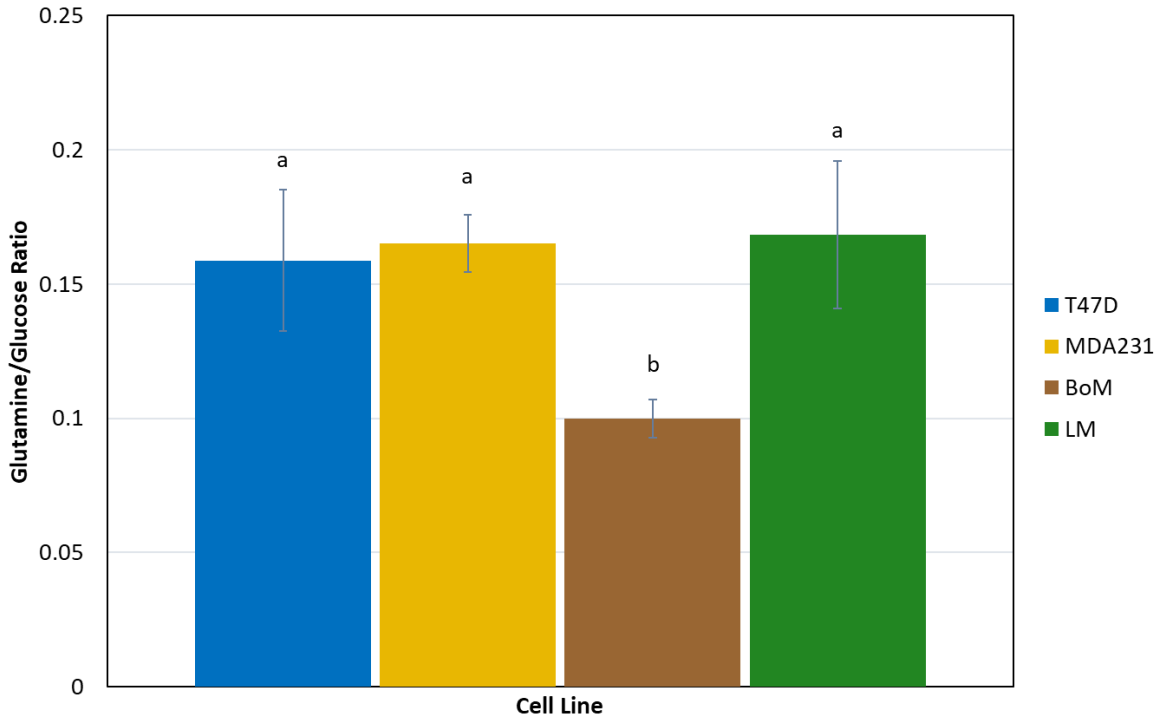

Figure 9: The glutamine to glucose ratio shown across cell lines with ^{13}C glutamine. The buffer concentration was determined by taking data from the previous graphs into a ratio. Rates were normalized to total SDS-soluble protein. Data are mean ± standard error (n=4). Within a treatment, means sharing the same letter are not significantly different. Asterisks above a letter denote significant difference with the corresponding cell line in glutamine-free buffer.

F. Protein content

From the 5 h pre-equilibration in experimental buffer through the three incubation periods used to assess glucose, lactate, and glutamine rates, cells were either treated without or with glutamine for approximately 11 h. Protein content was used as a measurement of total cell number to normalize all uptake rates. However, since the duration of these experiments was approximately 11 h, it was of interest to determine whether the presence of glutamine over this time period significantly affected the

proliferation of each cell line compared to the glutamine deprived controls. There was a significant increase in protein content of MDA231 ($p<0.01$) and BoM ($p=0.03$) lines given glutamine, whereas glutamine did not affect T47D and LM protein content. The effect on BoM cells was unexpected given this line had lower preference for glutamine relative to glucose than the other three lines (***Fig. 10***). Although there were significant differences within two cell lines, there was no significant main effect of glutamine on the protein content by 2-way ANOVA (***Table 1***). It should be noted that each line was seeded at 0.9-1.1 million cells per well for these experiments, so the expectation was that protein content should be similar between the lines. This was true for T47D, BoM, and LM cells, but the MDA231 content was significantly lower. This was attributed to the fact that MDA231 cells are known to adhere more loosely to cell culture wells, and not make cell-cell contacts due to poor expression of cadherins. Their weaker attachment was reflected in the cell pellets that were consistently recovered with this cell line following each incubation period (protein content in these pellets was quantitated to correct for this loss over each experiment). Thus, a significant number of MDA231 cells seeded in each well likely never attached and were washed from the well prior to the experiments.

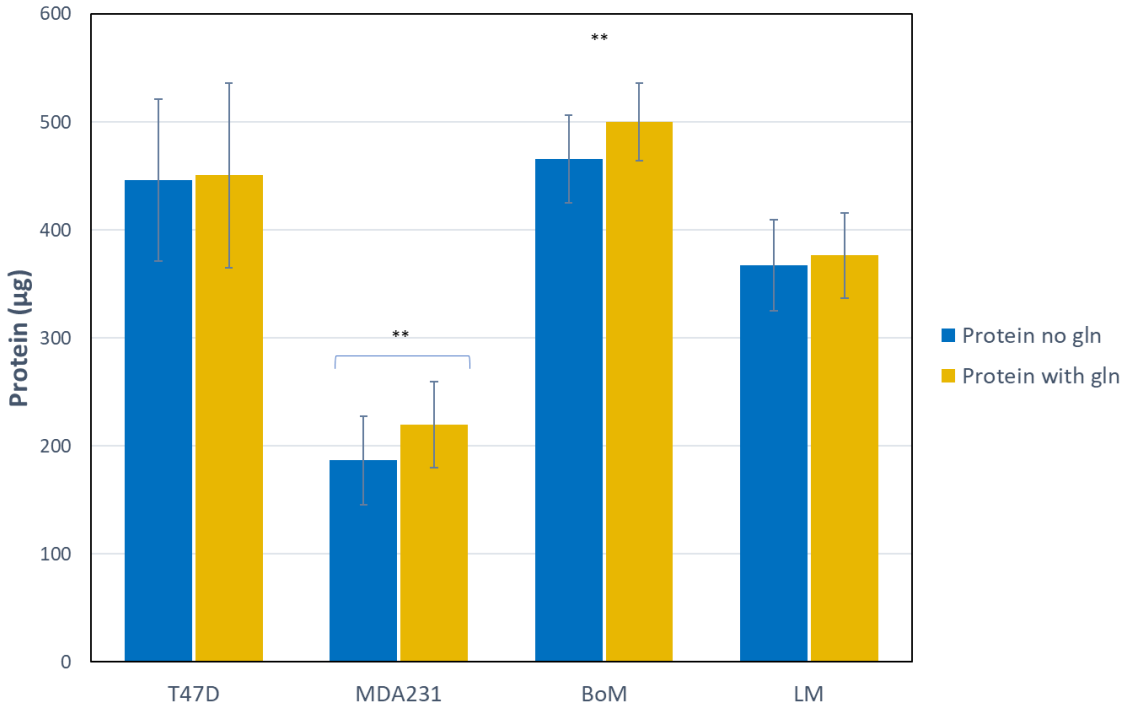

Figure 10: Protein concentration in soluble cell extracts for each cell line incubated with or without glutamine. Protein concentrations were determined through BCA assay averaged over two 60 min. incubations. SDS-soluble protein was used to normalize rates. Data are mean ± standard error (n=4). Within a treatment, means sharing the same letter are not significantly different. Asterisks above a letter denote significant difference with the corresponding cell line in glutamine-free buffer.

DISCUSSION

The overall goal of this research was to determine if metastatic sub-clones that preferentially invade and grow in lung or bone tissue exhibit metabolic differences from the parent MDA231 breast cancer line. Such metabolic plasticity may be important for tumor growth in different tissue microenvironments, and may guide development of tumor-specific, metabolic-targeted therapies. Potential metabolic differences were evaluated by quantifying (a) rates of glucose and oxygen consumption as well as lactate production, and (b) the rate of glutamine consumption, and the impact of exogenous glutamine on the measured rates and total protein content. Metabolic reprograming from a non-proliferative state is considered a hallmark of cancer that allows cells to redirect nutrients such as glucose and glutamine for anabolic reactions while maintaining ATP and redox homeostasis (15, 16). A major finding of this study is that the metabolic phenotypes differ between the LM and BoM sub-clones and the MDA231 parent line. The BoM and LM lines have a more aerobic glycolysis phenotype and less mitochondrial activity compared to MDA231 cells. Moreover, LM cells appear to differ from BoM cells in how they use glutamine. The data are consistent with further metabolic reprogramming as tumor cells metastasize to different tissues.

Glucose and glutamine are important substrates for production of ATP and metabolites necessary for many biosynthetic reactions to maintain cancer cell growth (17). Glucose is the main substrate, however many become dependent on glutamine for redox homeostasis

and fatty acid synthesis. Glucose is primarily metabolized through glycolysis to generate seven distinct three-carbon metabolites, the last of which is pyruvate. One of the first of these metabolites is glyceraldehyde-3-phosphate, which can be used to synthesize the pentose phosphate sugars through the non-oxidative pentose phosphate pathway. 3-phosphoglycerate, a key metabolite used for serine and glycine biosynthesis, is a second important metabolite generated by oxidation of glyceraldehyde-3-phosphate in two reactions that also yields the reduced cofactor NADH and ATP. NADH is the primary source of electrons used to reduce pyruvate to lactate but can additionally be transported into mitochondria through the malate-aspartate shuttle to provide electrons to the respiratory chain. The three reactions downstream of 3-phosphoglycerate include the enzyme pyruvate kinase that generates ATP and pyruvate from phosphoenolpyruvate. Pyruvate can be transaminated to form alanine or transported into mitochondria for complete oxidation for ATP synthesis or for fatty acid synthesis via the TCA cycle metabolite citrate (17).

Glutamine metabolism is important as an entry point of carbon to replenish some of the TCA cycle metabolites removed for anabolic reactions, but also serves as a substrate for ATP synthesis (18). Although glutamine is not required for the viability of cancer cells, it is important in allowing their continued proliferation by supporting protein, fatty acid, and ATP synthesis (15). Glutamine is deaminated into ammonia and glutamate the latter of which is oxidized into α-ketoglutarate (α-KG), that is further processed in the TCA cycle. α-KG can also be generated by transamination reactions of glutamate with pyruvate or other organic acids. The amino group from glutamine, whether released as free ammonia or transferred to other metabolites, can be used for nitrogen dispersal into

non-essential amino acids, hexosamines, and nucleotides, all of which are important for cell proliferation. Notably, glutamine can be used for cellular redox homeostasis as an indirect substrate for glutathione synthesis or through conversion to the TCA cycle metabolite malate, which is subsequently oxidized by malic enzyme to generate pyruvate and NADPH; this cofactor is an important source of electrons for protection against reactive oxygen species and for a number of biosynthetic reactions (17). A summary of these metabolic pathways can be found in the introductory figure (***Fig. 1***).

T47D is a luminal less malignant breast cancer subtype that proliferates slowly and has a low pathological grade amenable to chemo- and radiation therapies. In contrast, the MDA231 line is a malignant triple negative breast cancer of basal cellular origin that has an aggressive behavior with a poor prognosis once metastasis occurs (19). Highly metastatic behavior is typically associated with phenotypically different metabolisms (20). The results of this study support such a metabolic transformation with metastasis, as MDA231 cells exhibited approximately 3-fold greater consumption of both glucose and glutamine, as well as production of lactate. This is consistent with a previous study showing MDA231 exhibits 2-3 fold higher glucose consumption and lactate production than T47D cells (21). Higher glucose and glutamine consumption by MDA231 cells are likely driven by a combination of increased consumption of glycolytic and TCA cycle metabolites by a number of biosynthetic reactions and a higher overall ATP demand because of greater ATP-dependent biosynthesis flux. The fact that glutamine significantly increased MDA231 protein content while having no effect in T47D cells is consistent with this substrate being important for support of biosynthesis reactions. This is further supported by a recent report showing that glutamine enhances MDA231 growth (22).

MDA231 cells overexpress SLC1A5 and SLC7A5 amino acid transporters that drive glutamine uptake in a Na^+-dependent and independent manner, respectively (23). The fact that this uptake tended to lower glucose uptake, lactate production, the lactate: glucose ratio (aerobic glycolysis) and mitochondrial respiration rate of both T47D and MDA231 cells suggests that glutamine reduces overall cellular ATP production, and correspondingly ATP consumption. For MDA cells, this is difficult to reconcile with the fact that glutamine enhances total protein content and proliferation, which are expected to increase ATP consumption. One possible interpretation of these data is that a significant proportion of glutamine may be used for glutathione synthesis and redox homeostasis, which could indirectly offset higher biosynthesis-linked ATP consumption. Availability of glutathione is important for removal of hydrogen peroxide through glutathione peroxidase and protection of protein thiols through glutaredoxin, both of which help to maintain the cellular redox state. In doing so, the activities of the ubiquitin-proteasome system and autophagy/mitophagy pathways for removal of damaged proteins and mitochondria, both of which are ATP-dependent, could be reduced. Moreover, homeostasis of the cellular redox state through glutathione availability may increase the efficiency of mitochondrial oxidative phosphorylation (thereby increasing the ATP/O ratio) and/or reduce respiratory chain electron leak to oxygen to form superoxide. MDA231 cells have been found to be dependent on glutamine (22). The cells begin to undergo apoptosis after two days without glutamine; however, they can survive without glucose. This further supports the possibility that MDA231 cells use glutamine to synthesize glutathione. High reactive oxygen species (ROS) production that is not countered by adequate antioxidant defenses that include glutathione-dependent reactions

can lead to Bax activation, cytochrome c release, and caspase-mediated apoptosis. Glutamine may thus be important to MDA231 cells for both biosynthesis and defense against oxidative stress.

Importantly, glutamine did not reduce overall ATP consumption in LM and BoM cells. This could indicate that these cells have a lower ROS load, are less oxidatively stressed, and hence require less glutathione. However, higher ATP consumption is predicted in BoM cells given their modest but significantly greater protein content with glutamine; this could indicate a modest effect of glutamine on antioxidant defenses and therefore the proteasome-autophagy pathways. Notable, LM cell response to glutamine differed by stimulating mitochondrial respiration and reducing aerobic glycolysis with no effect on protein content. This suggests LM cells use glutamine primarily as a mitochondrial substrate for ATP synthesis; stimulation of oxidative phosphorylation secondarily lowers aerobic glycolysis through increasing the ATP/ADP ratio, a phenomenon known as the Pasteur effect. This implies no significant demand for glutathione synthesis and hence relatively low proteasome-autophagy activities. Further experiments are required to assess the proportion of glutamine used for glutathione synthesis and the extent of ATP consumption by the proteasome and autophagy pathways.

Unlike MDA, T47D does not require glutamine for cell proliferation and can survive without it. This supports how T47D is not an aggressive metastatic cell line. It has been shown to use NH_4Cl as an alternative nitrogen source in glutamine deprived media (24).

Lactate production demonstrates a shift towards glycolytic flux (20). If considered for our data it would presume that MDA has the highest glycolytic flux, followed by LM, then BoM and finally T47D. High glycolytic flux and glucose consumption are associated

with more aggressive metastatic lines and exhibit greater invasive behavior (20). MDA231 has the highest lactate production, glucose consumption and respiration rate which supports the aggressive nature of the cell line.

Lung and bone specific metastatic lines consumed glucose at significantly slower rates than MDA231 cells yet had equivalent rates of lactate production. Therefore, the LM and BoM lines shunt a higher proportion of glucose to lactate and have a more aerobic glycolytic phenotype. Conversely, this implies that the MDA line uses more glucose for purposes other than aerobic glycolysis. The oxidative and non-oxidative pentose phosphate pathways are two major pathways that consume glucose to yield ribose phosphates for nucleotide synthesis and NADPH for anti-oxidant defenses and redox homeostasis. Preferential glucose use for NADPH synthesis is consistent with higher ROS production by MDA cells and significant glutamine consumption for glutathione synthesis. Most ROS are derived from mitochondria, which are substantially more active in the MDA than LM and BoM lines. While it is tempting to speculate that the differences in respiration rate account for differences in oxidative stress, mitochondrial ROS production rate depends on a number of factors and is not simply a function of respiratory chain activity. Substrate availability has an important impact on ROS production, as substrate limited mitochondria tend to have more oxidized electron carriers that would yield lower superoxide production. In this respect, it is worth speculating that LM and BoM respiration rate may be low because mitochondria are substrate limited, possibly due to limited capacity for pyruvate and/or glutamine transport into the matrix. Such a limitation could explain a relatively lower use of glucose and glutamine in these cell lines for NADPH and glutathione synthesis. Low mitochondrial activity in both LM

and BoM lines could be an important metabolic adaptation allowing these lines to thrive in lung and bone tissue, respectively. In vivo, lung and bone have received the highest and lowest, respectively, mass-adjusted blood flows of all organs (***Table 2***). Oxygen availability in the lungs (P_{O2} approximately 100 mmHg) is much higher than the systemic tissues (P_{O2} approximately 20 mmHg) due to both the inordinately high blood flow and the close proximity of alveolar air high in oxygen content, and crucially is one factor that directly correlates with mitochondrial ROS production. LM growth in this high oxygen environment may thus depend on limiting ROS production by restricted mitochondrial substrate availability. Conversely, metabolically active BoM cells are expected to be in a oxygen-limited environment because of limited blood flow to bone. BoM cells may thrive in this environment because of gene expression changes that have minimized reliance on mitochondrial activity for ATP production; if this occurs by limiting substrate availability, a secondary consequence of this would be less ROS production.

Table 2: Comparison of mass-specific blood flow in different organs

Tissue	Blood flow (ml/min x 100 g tissue)	Reference
Bone	1.5-2.0	25
Dermis (skin)	4-10	26
Skeletal muscle	5-10	26
Intestine	30	26
Brain	57	26
Heart	70	26
Kidney	350	26
Lung	300-500	calculated

Conclusion

In summary, these results support the hypothesis that lung- and bone-specific metastatic subclones exhibit significantly different metabolic phenotypes than the parent MDA-MB-231 breast cancer line. The LM and BoM lines exhibited higher aerobic glycolysis and lower mitochondrial respiration than MDA231 cells. Lower mitochondrial activity may be important for LM adaptation to the high oxygen environment of the lungs to limit production of reactive oxygen species. Conversely, it may be important for BoM adaptation to the blood flow-limited environment of bone where restricted oxygen availability is likely. Glutamine was an important anabolic substrate for MDA231 and BoM cells, as total protein content was significantly increased compared to cells only given glucose; in contrast, LM cells preferentially oxidized this substrate in mitochondria. MDA231 aerobic glycolysis and respiration rate were lower with glutamine, which was surprising given that these cells had greater protein content. One possible explanation for this discrepancy is that MDA231 cells consume substantially more glutamine for glutathione synthesis and protection against oxidative stress. Taken together, growth of metastatic breast cancers in the lung and bone microenvironments are associated with reduced mitochondrial activity and higher aerobic glycolysis. Metabolic plasticity may thus be an important component to cancer metastasis.

REFERENCES

1. Minn, Andy J et al. Distinct organ-specific metastatic potential of individual breast cancer cells and primary tumors. The Journal of Clinical Investigation 115,1 (2005): 44-55. doi:10.1172/JCI22320
2. Gupta, G.P. et al. Identifying Site-Specific Metastasis Genes and Functions. Cold Spring Harbor symposia on quantitative biology. 70. (2005). 149-58. 10.1101/sqb.2005.70.018.
3. Bos, Paula D et al. Genes that mediate breast cancer metastasis to the brain. Nature. 459,7249 (2009): 1005-9. doi:10.1038/nature08021
4. Jia, Dongya et al. Elucidating cancer metabolic plasticity by coupling gene regulation with metabolic pathways. Proceedings of the National Academy of Sciences of the United States of America. 116,9 (2019): 3909-3918. doi:10.1073/pnas.1816391116
5. Devignes, Claire-Sophie et al. HIF signaling in osteoblast-lineage cells promotes systemic breast cancer growth and metastasis in mice. Proceedings of the National Academy of Sciences of the United States of America. 115,5 (2018): E992-E1001. doi:10.1073/pnas.1718009115
6. Arif, Tasleem et al. Mitochondrial VDAC1 Silencing Leads to Metabolic Rewiring and the Reprogramming of Tumour Cells into Advanced Differentiated States. Cancers. 10,12 499. 8 Dec. 2018, doi:10.3390/cancers10120499
7. Minn, Andy J et al. Genes that mediate breast cancer metastasis to lung. Nature. 436,7050 (2005): 518-24. doi:10.1038/nature03799
8. Kang, Yibin et al. Multigenic Program Mediating Breast Cancer Metastasis to Bone. Cancer Cell 3: (2003) 537-549. 10.1016/S1535-6108(03)00132-6.
9. Pavlova, Natalya N, et al. The Emerging Hallmarks of Cancer Metabolism. Cell metabolism. 23,1 (2016): 27-47. doi:10.1016/j.cmet.2015.12.006
10. Daye, Danie et al. Metabolic Reprogramming in Cancer: Unraveling the role of Glutamine in Tumorigenesis. Seminars in Cell & Developmental Biology. 23,4 (2012): 362-369.
11. DeBerardinis, Ralph J et al. Fundamentals of Cancer Metabolism. Science advances. 2,5 e1600200. 27 May. 2016, doi:10.1126/sciadv.1600200
12. LM: Minn AJ, Gupta GP, Siegel PM, Bos PD, Shu W, Giri DD, Viale A, Olshen AB, Gerald WL, Massagué J Genes that Mediate Breast Cancer Metastasis to Lung. Nature, 436, (2005) 518-524.

13. BoM: Kang Y, Siegel PM, Shu W, Drobnjak M, Kakonen SM, Cordón-Cardo C, Guise TA, Massagué J A Multigenic Program Mediating Breast Cancer Metastasis to Bone. Cancer Cell, 3, (2003) 537-549.
14. Meijer T.W.H., Peeters W.J.M., Dubois L.J., van Gisbergen M.W., Biemans R., Venhuizen J.-H., Span P.N., Bussink J. Targeting Glucose and Glutamine Metabolism Combined with Radiation Therapy in Non-Small Cell Lung Cancer. Lung Cancer, 126, (2018) 32-40.
15. Boroughs, Lindsey K, and Ralph J DeBerardinis. Metabolic Pathways Promoting Cancer Cell Survival and Growth. Nature cell biology. 17,4 (2015): 351-9. doi:10.1038/ncb3124
16. Hudson, Chantelle D et al. Altered Glutamine Metabolism in Platinum Resistant Ovarian Cancer. Oncotarget. 7,27 (2016): 41637-41649. doi:10.18632/oncotarget.9317
17. Hirschey, Matthew D et al. Dysregulated Metabolism Contributes to Oncogenesis. Seminars in cancer biology. 35 Suppl (2015): S129-S150. doi:10.1016/j.semcancer.2015.10.002
18. Jiang, Zi-Feng et al. Hypoxia Promotes Mitochondrial Glutamine Metabolism Through HIF1α-GDH Pathway in Human Lung Cancer Cells. Biochemical and Biophysical Research Communications. 483 (2017): 32-38.
19. Xiao, Wenjun et al. The Frequency of CpG and Non-CpG Methylation of Notch3 Gene Promoter Determines its Expression Levels in Breast Cancer Cells. Experimental Cell Research. 386 (2020): 111743.
20. Jung, Kyung-Ho et al. EGF Receptor Stimulation Shifts Breast Cancer Cell Glucose Metabolism Toward Glycolytic Flux Through PI3 Kinase Signaling. PloS one. 14,9 e0221294. 18 Sep. 2019, doi:10.1371/journal.pone.0221294
21. Bartmann, Catharina et al. Beta-hydroxybutyrate (3-OHB) can Influence the Energetic Phenotype of Breast Cancer Cells, but Does not Impact Their Proliferation and the Response to Chemotherapy or Radiation. Cancer & metabolism. 6 8. 11 Jun. 2018, doi:10.1186/s40170-018-0180-9
22. Ocaña, M.C.; Martínez-Poveda, B.; Quesada, A.R.; Medina, M.Á. Glucose Favors Lipid Anabolic Metabolism in the Invasive Breast Cancer Cell Line MDA-MB-231. Biology 2020, *9*, 16.
23. Cha, Yoon Jin et al. Amino Acid Transporters and Glutamine Metabolism in Breast Cancer. International journal of molecular sciences. 19,3 907. 19 Mar. 2018, doi:10.3390/ijms19030907
24. Lie, Shervi et al. The Ability to Utilise Ammonia as Nitrogen Source is Cell Type Specific and Intricately Linked to GDH, AMPK and mTORC1. Scientific reports. 9,1 1461. 6 Feb. 2019, doi:10.1038/s41598-018-37509-3
25. Heinonen, I., Kemppainen, J., Kaskinoro, K., Langberg, H., Knuuti, J., Boushel, R., Kjaer, M., and Kalliok, K. Bone Blood Flow and Metabolism in Humans: Effect of Muscular Exercise and Other Physiological Perturbations. J. Bone Miner. Res. 28(5), 1068-1074, 2013
26. Patton, H.D., Fuchs, A.F., Hille, B., Scher, A.M., and Steiner, R. (Editors). Textbook of Physiology, 21st Edition, W.B. Saunders Co., 1989.